

## Evolution of the active surface of the vanadyl pyrophosphate catalysts

V.V. Guliants, J.B. Benziger<sup>1</sup>, S. Sundaresan, N. Yao

*Princeton Materials Institute, Princeton University, Princeton, NJ 08544, USA*

and

I.E. Wachs

*Zettlemoyer Center for Surface Studies, Lehigh University, Bethlehem,  
PA 18015, USA*

Received 11 January 1995; accepted 23 February 1995

Bulk crystallinity of vanadyl(IV) pyrophosphate catalysts for *n*-butane partial oxidation increased up to 23 days on stream as determined by XRD and Raman spectroscopy, while selectivity reached steady state after 8–10 days. Electron microscopy detected a 15 Å amorphous layer terminating the (200) planes of  $(\text{VO})_2\text{P}_2\text{O}_7$  in fresh catalysts that was not observed in the equilibrated catalysts. It is suggested that ordering of (200) planes at the surface of  $(\text{VO})_2\text{P}_2\text{O}_7$  is responsible for selective oxidation.

**Keywords:** VPO catalysis; vanadyl(IV) pyrophosphate; high resolution electron microscopy; surface

Vanadium–phosphorus oxides (VPO) have been used for the selective oxidation of *n*-butane since the mid 1970's, and the nature of the active catalyst has been the object of extensive research [1]. Many crystalline phases exist in the VPO system and correlations of catalytic activity with crystalline structure have been reviewed [1,2]. Vanadyl(IV) pyrophosphate,  $(\text{VO})_2\text{P}_2\text{O}_7$ , has been identified as critical for the selective oxidation of *n*-butane [2]. Vanadyl pyrophosphate is prepared from the precursor, vanadyl(IV) hydrogen phosphate hemihydrate,  $\text{VOHPO}_4 \cdot 0.5\text{H}_2\text{O}$ . Calcination in nitrogen causes loss of water and the transformation of the hemihy-

<sup>1</sup> To whom correspondence should be addressed.

hydrate into the pyrophosphate [1]. The precursor can be prepared from either aqueous or alcoholic solutions. The choice of preparation medium alters the morphology of the hemihydrate and in turn the composition and morphology of the final VPO catalyst, ultimately determining the catalyst performance [3].

X-ray diffraction has been the principal tool to characterize the VPO catalysts. In the best catalysts vanadyl pyrophosphate has been the only crystalline phase identified [1]. Spectroscopic probes, especially Raman spectroscopy, have supplemented XRD and have shown that the VPO catalyst is only partially crystalline and contains amorphous and/or other crystalline phases [4]. Several investigators have suggested that vanadyl pyrophosphate acts as a support for amorphous or other crystalline phases, and these surface phases are the source of selective oxidation catalysis [5–7]. Our recent work has shown that the presence of microcrystalline vanadyl(V) orthophosphates, presumably supported on the surface of vanadyl pyrophosphate, degraded the catalyst performance [8]. An amorphous VPO component generated from vanadyl(IV) dihydrogen phosphate,  $\text{VO}(\text{H}_2\text{PO}_4)_2$ , also resulted in inferior catalyst performance [8]. The best catalysts contained only  $(\text{VO})_2\text{P}_2\text{O}_7$ , with well-ordered stacking of the (200) planes [8]. However, until now no microscopic studies of surface termination of the (200) planes have been reported.

In the present study the specific termination of model VPO catalyst surfaces has been observed with HREM and compared with XRD, Raman spectroscopy, and *n*-butane oxidation kinetics to determine if the specific catalyst microstructure can be associated with the selective oxidation catalysis.

Model VPO catalysts were prepared by reacting vanadium pentoxide (Aldrich) with excess aqueous phosphoric acid (Fisher) to produce vanadyl(V) orthophosphate dihydrate,  $\text{VOPO}_4 \cdot 2\text{H}_2\text{O}$  [9]. The dihydrate was then reduced to the hemihydrate precursor by refluxing in 2-butanol (Aldrich) for 24 h. The hemihydrate was calcined at 823 K in flowing nitrogen for 2 h [10], producing fresh model vanadyl pyrophosphate catalyst platelets ca.  $5 \times 0.2 \mu\text{m}^2$ .

Kinetic measurements were carried out on ca. 1 g of the 212–355  $\mu\text{m}$  fraction of fresh catalyst in 1.2% *n*-butane in air at 653 K for up to 23 days. The feed flow-rate was fixed at 30 ml/min to yield a once-through *n*-butane conversion of 25%. The kinetic measurements and the analysis of products by gas chromatography were described in detail elsewhere [8]. The used catalyst after kinetic experiments was characterized by XRD and Raman.

A sample of the fresh catalyst in powder form was also placed in a tubular oven and kept under the same reaction conditions as in the kinetic measurements. Samples were removed periodically from the tubular oven and characterized by X-ray diffraction, Raman spectroscopy and HREM. The details of the XRD and Raman experiments are reported elsewhere [8].

For HREM, the powdered VPO catalyst samples were embedded in epoxy resin, cut to 50–70 nm and deposited from dimethylsulfoxide onto a holey carbon film. During preliminary experiments the VPO catalysts were found to be electron

beam-sensitive, and embedding the catalyst particles in epoxy resin prior to sectioning improved the stability under the electron beam. HREM studies were carried out in a Phillips CM-20 TEM/STEM electron microscope operating at 200 kV and residual pressure of ca.  $10^{-7}$  Torr.

The platelet morphology of the model VPO catalysts is clear in the scanning electron micrograph shown in fig. 1. The basal faces correspond to the (200) planes of vanadyl pyrophosphate, while the side faces represent other planes (e.g. 001, 021, and  $02\bar{1}$ ) which have been suggested as unselective in hydrocarbon oxidation [11]. XRD analysis and Raman spectroscopy show the precursor to be  $\text{VOHPO}_4 \cdot 0.5\text{H}_2\text{O}$ , and after calcination in nitrogen only  $(\text{VO})_2\text{P}_2\text{O}_7$ , is identified. The crystalline order of vanadyl pyrophosphate evolved with time on-stream in the butane–air feed. At no time during the entire activation period on stream did the XRD and Raman spectra detect VPO phases other than  $(\text{VO})_2\text{P}_2\text{O}_7$ . The full width at half maximum (FWHM) of the (200) reflection in the XRD pattern and intensity of the P–O–P asymmetric stretch of vanadyl pyrophosphate at  $921\text{ cm}^{-1}$  [12] were used as a measure of, respectively, long and short range order in the  $(\text{VO})_2\text{P}_2\text{O}_7$  catalyst. Fig. 2 shows the increase in Raman intensity of the  $921\text{ cm}^{-1}$  band over a period of 23 days, along with the selectivity to maleic anhydride at constant feed flowrate through the reactor. The selectivity to maleic anhydride rose during the first 8–10 days and then leveled off. Both the FWHM of the (200) reflection and Raman  $921\text{ cm}^{-1}$  band intensity changed even after 10 days indicating that the

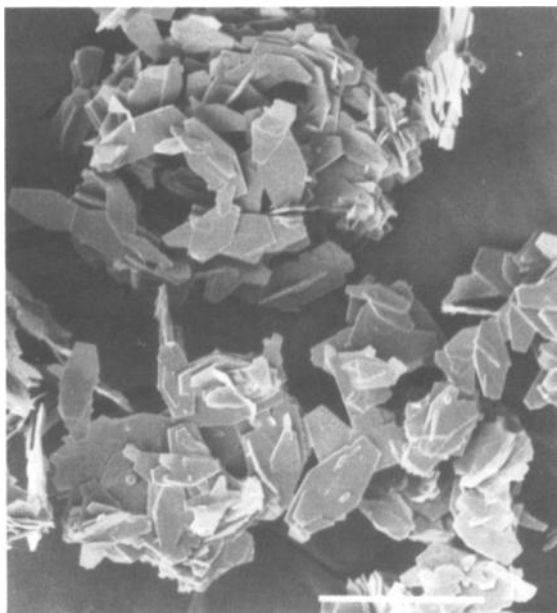


Fig. 1. SEM micrograph of model organic VPO catalyst. The bar corresponds to  $10\text{ }\mu\text{m}$ .

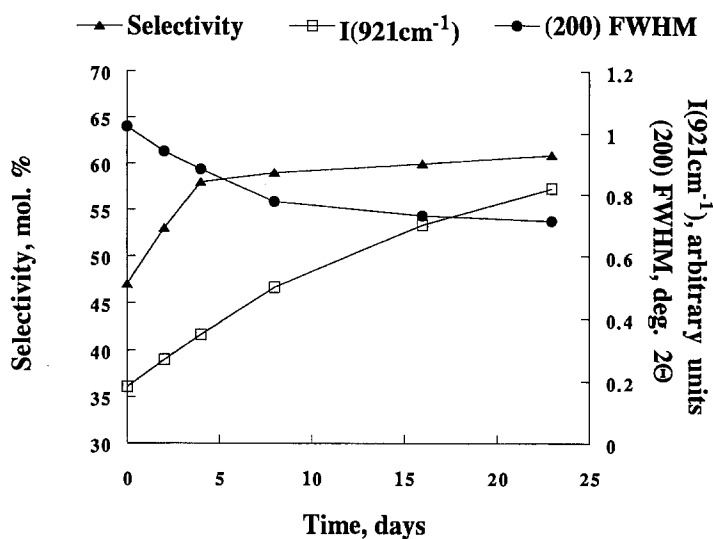


Fig. 2. Evolution of the bulk crystallinity and selectivity of vanadyl pyrophosphate catalyst to maleic anhydride (mol%) with time under catalytic conditions at 653 K in 1.2% *n*-butane–air feed at 25 mol% *n*-butane conversion.

ordering in the bulk continued beyond surface equilibration. The areas of  $921\text{ cm}^{-1}$  peak paralleled the behavior of the intensity of the  $921\text{ cm}^{-1}$  band confirming continuing process of local crystallization. The used catalyst after the kinetic measurements also contained only  $(\text{VO})_2\text{P}_2\text{O}_7$  by XRD and Raman of crystallinity similar to that of the in situ sample after 23 days.

Representative high resolution electron microscopy images of the fresh catalyst, and the catalysts after 8 and 23 days under catalytic conditions are shown in figs. 3a–3c, respectively. The high resolution images display a series of parallel lines, or a fringe pattern. The spacing between the fringes was  $3.8\text{ \AA}$ , corresponding to the spacing between the (200) planes of  $(\text{VO})_2\text{P}_2\text{O}_7$  [13]. Careful examination of the surface region of the micrographs shows the fresh catalyst is terminated in a thin, ca.  $15\text{ \AA}$ , amorphous region. This amorphous region contracts to ca.  $5\text{ \AA}$  in catalyst after 8 days in the reactor, whereas the (200) planes extend up to the last surface layer in the equilibrated catalysts (23 days in the reactor). The crystallization of the vanadyl pyrophosphate surface coincided with much higher steady state selectivity to maleic anhydride.

Crystallization of the surface region took place under reaction conditions over a period of weeks while reaction selectivity for partial oxidation improved. Many studies have reported the performance of the VPO catalysts correlated with the degree of bulk crystallinity [6,8,10]. We show here, that the crystalline ordering in the surface region correlates better with catalyst performance. It has been suggested that the excess phosphate employed in the precursor synthesis terminated the surface with pyrophosphate groups [14]. These pyrophosphate groups may pre-

vent chemisorbed oxygen species from migrating across the active surface and create so-called site isolation of vanadyl dimers proposed for selective hydrocarbon oxidation [14].

The VPO system is complex. Different preparation routes lead to the same bulk vanadyl(IV) pyrophosphate phase, but relative exposure of the selective (200) planes [11] and the surface termination are different. An amorphous layer which terminates the surface was observed on fresh catalysts and disappeared with time on stream leading to high steady state performance.

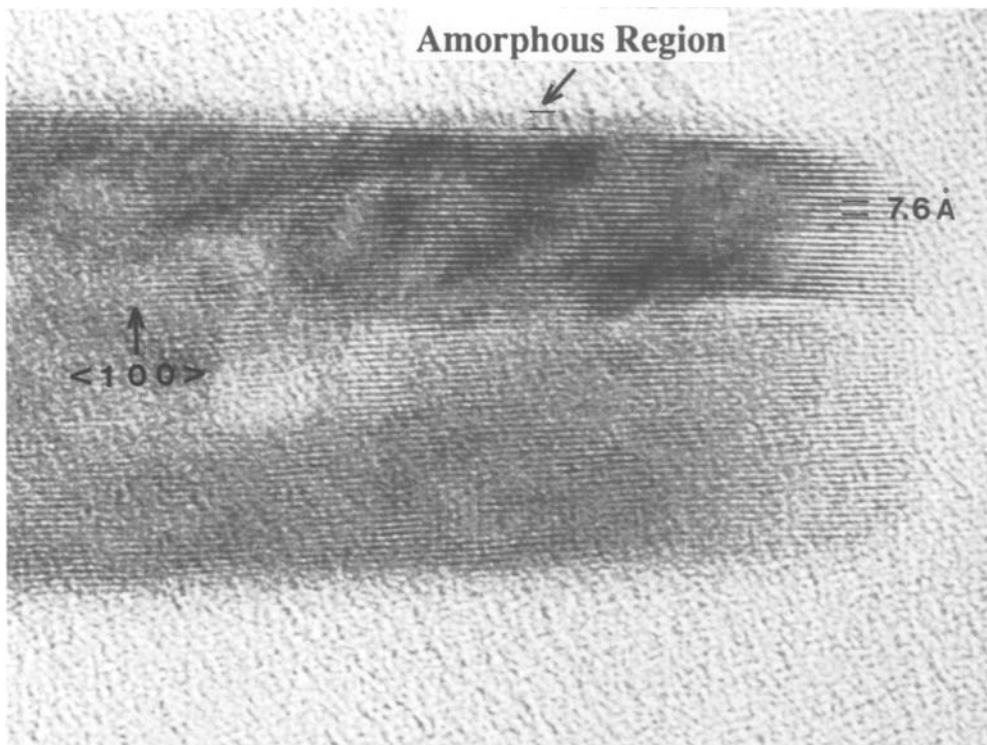


Fig. 3. HREM micrographs of the model VPO catalysts at magnification 300 000. (a) The micrograph of the fresh model organic VPO catalyst taken along the  $\langle 001 \rangle$  axis of  $(\text{VO})_2\text{P}_2\text{O}_7$ . An arrow indicates amorphous VPO layer. (b) The micrograph of the model organic VPO catalyst after 8 days under catalytic conditions. Same imaging conditions as in (a). (c) The micrograph of the model organic VPO catalyst after 23 days under catalytic conditions. Same imaging conditions as in (a).

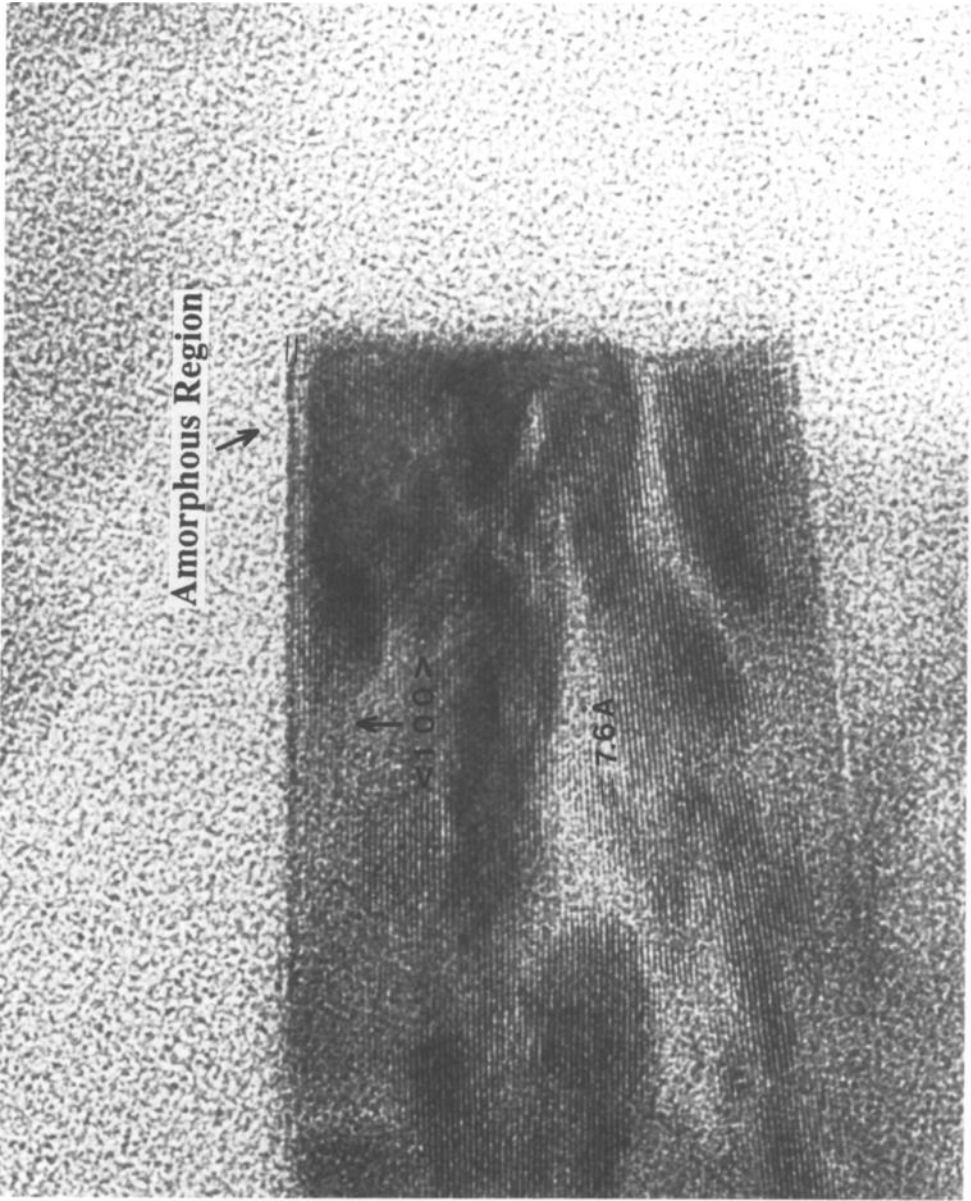


Fig. 3. Continued.

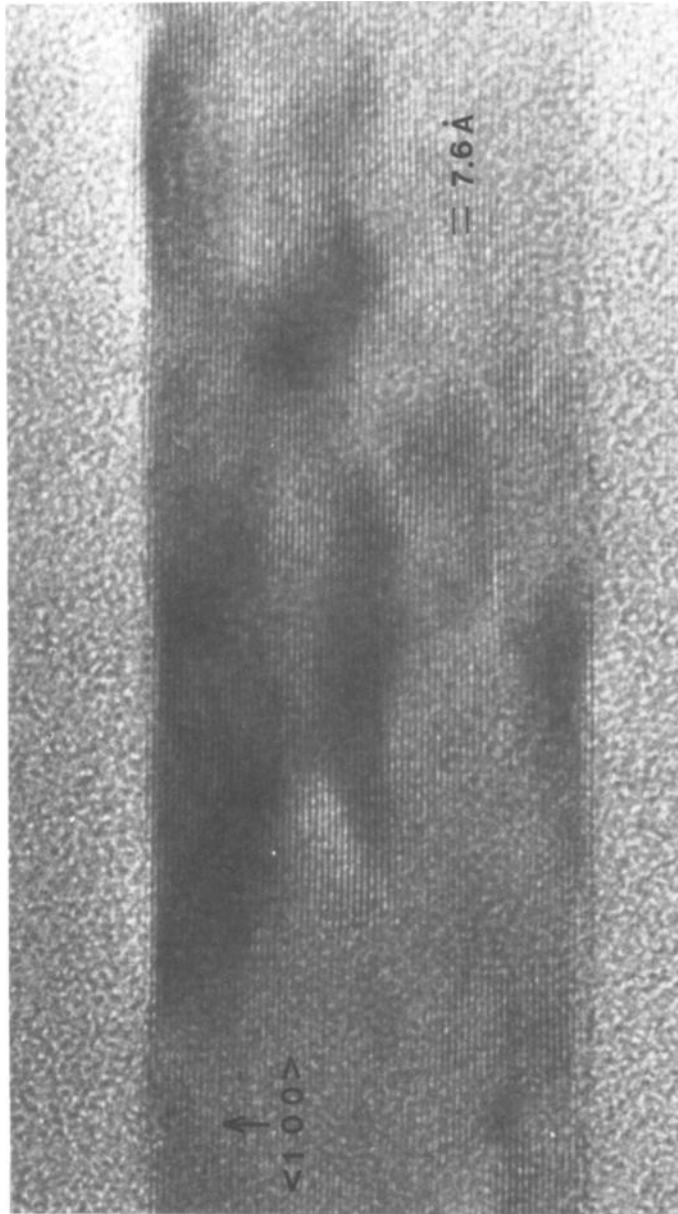


Fig. 3. Continued.

## Acknowledgement

The authors are grateful to J.G. Goodhouse of Princeton University for HREM sample preparation. This work was supported by the Amoco Chemical Corporation and National Science Foundation Grant CTS-9100130.

## References

- [1] G. Centi, F. Trifirò, J.R. Ebner and V.M. Franchetti, *Chem. Rev.* 88 (1988) 55.
- [2] G. Centi, *Catal. Today* 16 (1993) 5.
- [3] H.S. Horowitz, C.M. Blackstone, A.W. Sleight and G. Teufer, *Appl. Catal.* 38 (1988) 193.
- [4] N. Harrouch Batis, H. Batis, A. Ghorbel, J.C. Vedrine and J.C. Volta, *J. Catal.* 128 (1991) 248.
- [5] E. Bordes, *Catal. Today* 1 (1987) 499.
- [6] H. Morishige, J. Tamaki, N. Miura and N. Yamazoe, *Chem. Lett.* (1990) 1513.
- [7] *Catal. Today* 16 (1993), special issue on VPO catalysis.
- [8] V.V. Guliants, J.B. Benziger, S. Sundaresan, I.E. Wachs and J.-M. Jehng, *J. Catal.*, submitted.
- [9] G. Ladwig, *Z. Anorg. Allg. Chem.* 338 (1965) 266.
- [10] H. Igarashi, K. Tsuji, T. Okuhara and M. Misono, *J. Phys. Chem.* 97 (1993) 7065.
- [11] F. Cavani and F. Trifirò, *Catal.* 11 (1994) 246.
- [12] T.P. Moser and G.L. Schrader, *J. Catal.* 92 (1985) 216.
- [13] G. Centi, F. Trifirò, G. Busca, J. Ebner and J. Gleaves, *Faraday Discussions Chem. Soc.* 87 (1989) 215.
- [14] J.R. Ebner and M.R. Thompson, in: *Structure-Activity and Selectivity Relationships in Heterogeneous Catalysis*, eds. R.K. Grasselli and A.W. Sleight (Elsevier, Amsterdam, 1991) p. 31.